Pressing and Sintering of Titanium Aluminide Powder after Ball Milling in Silane-Doped Atmosphere

Bernd-Arno Behrens , Kai Brunotte , Julius Peddinghaus , Jonathan Ursinus , Sebastian Döring * , Wolfgang Maus-Friedrichs , René Gustus , Maik Szafarska *

Posted Date: 12 July 2023

doi: 10.20944/preprints202307.0801.v1

Keywords: Die pressing and sintering; powder metallurgical process; titanium aluminide powder

Article

Pressing and Sintering of Titanium Aluminide Powder after Ball Milling in Silane-Doped Atmosphere

Bernd-Arno Behrens [1], Kai Brunotte [1], Julius Peddinghaus [1], Jonathan Ursinus [1], Sebastian Döring [1,*], Wolfgang Maus-Friedrichs [2], René Gustus [2] and Maik Szafarska [2,*]

[1] Leibniz Universität Hannover, Institut für Umformtechnik und Umformmaschinen, 30823 Garbsen, Deutschland, behrens@ifum.uni-hannover.de (B.-A.B.); brunotte@ifum.uni-hannover.de (K.B.), peddinghaus@ifum.uni-hannover.de (J.P.), ursinus@ifum.uni-hannover.de (J.U.), s.doering@ifum.uni-hannover.de (S.D.)

[2] Technische Universität Clausthal, Clausthaler Zentrum für Materialtechnik, 38678 Clausthal Zellerfeld, Deutschland, maik.szafarska@tu-clausthal.de (M.S.), rene.gustus@tu-clausthal.de (R.G.), wolfgang.maus-friedrichs@tu-clausthal.de (W.M.-F.)

* Correspondence: s.doering@ifum.uni-hannover.de; +49 (0) 511 762 4106; maik.szafarska@tu-clausthal.de; +49 (0) 5323 723374

Abstract: Due to the high specific surface area of titanium aluminide powders, significant and unavoidable surface oxidation takes place during processing. The resulting oxides disrupt the conventional powder metallurgical process route (pressing and sintering) by reducing green strength and sintered properties. Oxide-free particle surfaces offer the potential to significantly increase particle bond strength and enable the processing of difficult-to-press material powders. In this work, the effect of milling titanium aluminide powder in a silane-doped atmosphere on the component properties after pressing and subsequent sintering was investigated. Ball milling was used to break up the oxide layers and create bare metal surfaces on the particles. With the help of silane-doped inert gas, the oxygen partial pressure was greatly reduced during machining. It was investigated whether oxide-free surfaces could be produced and maintained by milling in silane-doped atmospheres. Furthermore, the resulting material properties after pressing and sintering were analyzed using density measurements, hardness tests, EDX-measurements and micrographs. It was concluded, that ball milling in a silane-doped atmosphere produces and maintains oxide-free particle surfaces. These oxide-free surfaces and smaller particle sizes improve the component properties after pressing and sintering.

Keywords: Die pressing and sintering; powder metallurgical process; titanium aluminide powder

1. Introduction

Titanium aluminides (TiAl) are intermetallic materials and γ-alloys in particular offer great application potential in automotive and aerospace applications [1]. Whenever good creep resistance combined with low density at high operating temperatures is required, TiAl alloys with a density of only 3.9-4.2 g/cm³ represent a lighter alternative to titanium or nickel-based alloys. The properties of TiAl materials essentially depend on the microstructure, which in turn is determined by the alloy and the manufacturing and processing methods [2].

In order to improve the chemical and microstructural homogeneity compared to cast starting material, TiAl alloys are predominantly processed powder-metallurgically [3]. After the starting powder has been produced by inert gas atomisation, it is solidified by hot isostatic pressing (HIP) [4]. Subsequently, it is shaped by isothermal forging [5]. Alternatively, the component geometry is

 doi:10.20944/preprints202307.0801.v1

created directly from powder using the modified sintering processes Field Assisted Sintering (FAST) [6].

HIP, isothermal forging and FAST are demanding processes with high technical complexity. In contrast, die pressing and sintering have established themselves as a cost-effective and productive near-net-shape process for many other metallic powder materials [7]. However, when processing TiAl powder via the conventional process route, the low ductility of the particles poses a challenge. In addition, the oxide layers present make processing difficult.

Titanium aluminides have a high affinity for oxygen, which influences the microstructure development and thus the technological properties [8]. Interstitially resolved oxygen leads to an increased strain hardening of the powder, which reduces the compressibility during pressing and only weak surface contacts can be built up [9]. Furthermore, oxide layers consisting of titanium and aluminium oxides as well as mixed oxides build on the particle surfaces [10]. In die pressing, a strong bond is to be produced by cold welding the powder particles [11]. However, the existing oxide layers hinder the interlocking and the cold welding [12]. This leads to a reduction in compressibility and thus to reduced green strength [13]. During sintering, the oxide layers act as a diffusion barrier and therefore cause high porosities. They also reduce the thermal conductivity and the sinterability of powders [14]. This results in the formation of inhomogeneities in the microstructure [15].

TiAl powders react with oxygen when exposed to air, even at ambient temperatures, and should be processed under inert gas atmospheres to prevent an undesirable increase in the oxygen content of the powder particles [16]. However, in most inert gas atmospheres such as argon, the residual oxygen content is too high and must be reduced [17].

This is where the present study comes in by using silane-doped argon as the process atmosphere. Silane reacts with the residual oxygen of argon 5.0, which is about 2 ppm_v, and thus enables very low oxygen concentrations well below 10^{-20} ppm_v [18,19]. Now, existing oxide layers can be broken up by ball milling in and oxide-free particle surfaces are produced. The formation of new oxide layers on these bare surfaces can be prevented in this way. It is investigated whether and under which conditions a qualification of the conventional powder metallurgical process route (pressing and sintering) for titanium aluminide materials can be achieved by processing in this extremely low-oxygen atmosphere.

2. Materials and Methods

The study was carried out on TiAl powder of alloy GE48 (composition in wt.%: 59.60 Ti, 33.00 Al, 2.60 Cr and 4.80 Nb). The powder was produced by inert gas atomisation with argon and has a spherical shape. The D90 value (maximum particle size of 90 % of the volume of the initial powder) was 134 µm and the oxygen concentration of the powder was 909 ppm_w.

In a glovebox (GS Glovebox Systemtechnik GmbH), the GE48 powder was filled into the ball milling containers (FRITSCH GmbH, 250 ml, hardened steel DIN EN 10027-1 X105CrMo17) under an argon-silane atmosphere at an oxygen partial pressure below 1 x 10^{-18} ppm_v. Two containers were filled with 40 g of powder each and 345 g of milling steel balls (X105CrMo17) with a diameter of 10 mm and sealed gas-tight. The weight ratio of the steel balls and powder was chosen according to Murty et al. [20]. To minimise agglomeration due to cold welding, 12 drops of toluene were added [21]. The ball milling process was carried out with a Pulverisette 5/4 planetary ball mill (FRITSCH GmbH) at a speed of 300 1/min. Following Shengguan et al., where a relative density of 96 % was achieved after sintering by milling TiAl powder, an effective milling time of 5 h was set with an interruption of 4 min cyclically after every 3 min of active ball milling [22]. To avoid excessive heating of the milling vessels and to maintain stable process conditions, a further break of 10 min was taken after every 5 cycles.

After ball milling, the containers were reopened in the glove box with the oxygen-free atmosphere described above. The atmospheric and compacting conditions were varied to detect the effects of atmospheric conditions on this conventional powder metallurgical processing route. Table 1 shows an overview of the different sample variants. The variants XHV6 and XHV8 were compacted without contact with ambient air at two different compaction pressures. For further tests, the

Preprints (www.preprints.org) | NOT PEER-REVIEWED | Posted: 12 July 2023 doi:10.20944/preprints202307.0801.v1

compression pressure was kept constant (800 MPa). The V8 variant was subjected to vacuum drying in the airlock of the glove box in a silane-doped atmosphere in order to evaporate any toluene residue. In addition to creating the desired oxide free surface areas, the milling process also reduces the particle size of the powder. In order to assess the effect of the oxide surface conditions isolated from the effect of the particle size, additional reference samples were created with powder, exposed to ambient air after milling (L85 and L840). Variant REF represents the untreated reference with the particle size and shape before milling. Compaction to green bodies of 7 g and 20 mm diameter was done by one-sided pressing with a manually driven hydraulic press (MSE Teknoloji) in the glove box.

Table 1. Processing variants of the GE48 powder.

Designation	Pressure in MPa	Treatment
XHV6	600	Ball milled
XHV8	800	Ball milled
V8	800	Vacuum drying
L85	800	5 min. in air
L840	800	40 min. in air
REF	800	Untreated

Later, all green compacts were sintered in a hot tube furnace (Thermconcept ROC) at 1300 °C for 60 min. The temperature is based on previous FAST experiments achieving a desireable lamellar microstructure at this temperature [23]. The furnace is directly connected to the glove box via a cooled flange and is supplied with the oxygen-free atmosphere of the glove box via a fan (see Figure 1).

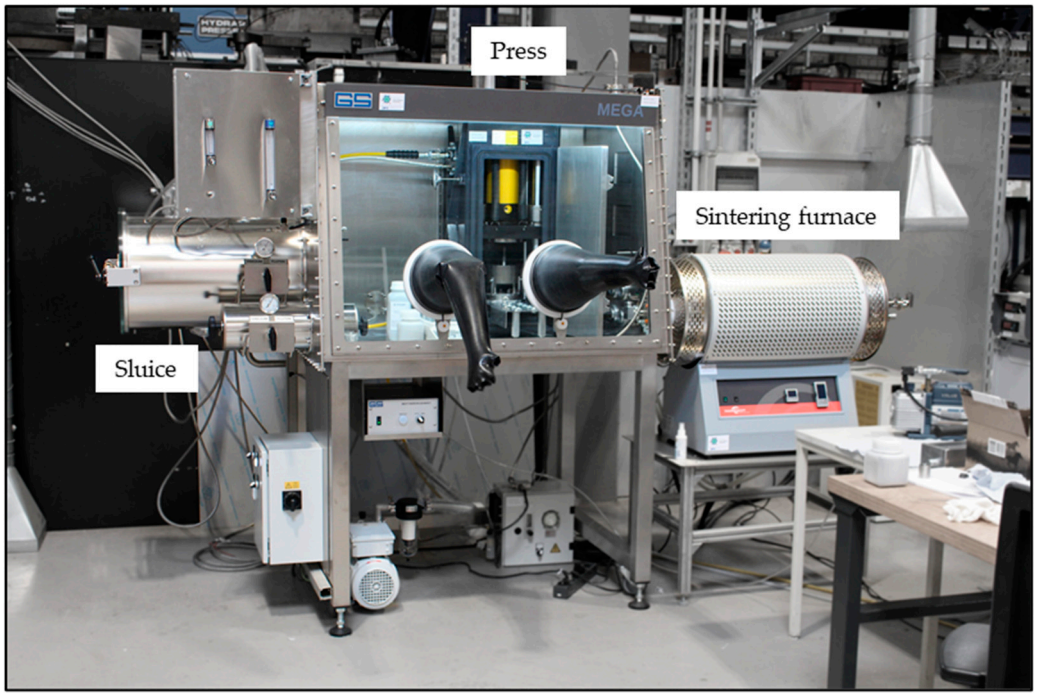

Figure 1. Structure of the glove box with press and sintering furnace.

For each process step, an analysis of the powder or sample was carried out. In order to investigate the influence of the particle size on the microstructure after ball milling, the particle size distributions of the milled and unmilled powders were determined. The measurement was carried out with a laser diffraction measuring system (HELOS, Sympatec). With the measuring system, the particle size can be determined in a measuring range from 0.1 µm to 8,750 µm. The characterisation of the elemental composition as well as the chemical state of the particle surface was carried out by X-ray photoelectron spectroscopy (XPS) with an information depth of about 10 nm in a modified

Preprints (www.preprints.org) | NOT PEER-REVIEWED | Posted: 12 July 2023 doi:10.20944/preprints202307.0801.v1

UHV (ultra-high vacuum) apparatus (VG ESCALAB MKII) with a base pressure of $2x10^{-10}$ mbar. Between the ball milling process and the measurement, the TiAl powder milled in a silane-doped atmosphere had no contact with the surrounding atmosphere due to a special transport system [24]. With the help of XPS measurement, the newly formed surfaces of the powder particles were examined with regard to oxidation. In XPS, X-rays are focused on the sample surface, where electrons are emitted due to the photoelectric effect. These photoelectrons have characteristic kinetic energies that correspond to the binding energy of their respective original orbital, which in turn is also influenced by the chemical state of the element involved. With the help of a hemispherical electron energy analyser, the electrons can be sorted according to their energy, which enables the presentation of a photoelectron spectrum. Non-monochromatic Al-Kα radiation (1486.6 eV) was used for XPS measurements generated in an XR40B X-ray source from PREVAC GmbH. The electron-pass energy was set to 100 eV for survey spectra and to 20 eV for detail spectra. Spectral analysis was performed using CASAXPS software from Casa Software Ltd. The spectra were recorded relative to the Fermi level and fitted with the algorithm developed by Levenberg-Marquard, which takes into account photoelectric cross sections according to Scofield and asymmetry parameters from Reilman et al [25,26]. Transport and transfer of the oxygen-free powder from the silane-doped argon atmosphere into the UHV chamber was carried out using a validated transfer system described by Gustus et al [24]. The other powders that were exposed to air were prepared in the conventional way with an airlock and transferred to the XPS instrument.

The green compacts were analysed optically after cold pressing of the prepared powders. It was investigated whether a compact green compact could be produced at all, which would be the basis for the sintering process. These green compacts were examined for cracks and fragmentation.

After sintering, the density of the samples was determined by weighing them in distilled water according to the Archimedes principle with a suitable measuring set-up (Sartorius YDK). Metallographic examinations of the sintered samples (Polyvar MET microscope) were carried out on longitudinal sections of the samples without etching and used for qualitative evaluation of the particle composite and the defect structure. EDX examinations (Zeiss Supra 55 VP) were carried out for phase determination. The hardness of the sintered bodies was determined according to Vickers HV1 with a Qness Q10A hardness tester.

3. Results

3.1. Particle Size Distribution

There was a significant reduction in particle size distribution after 5 hours of ball milling. The D90 value after milling was 53 µm. This corresponds to a reduction of the particle size to approx. 40%. A detailed representation of the particle size distributions is shown in Figure 2. A narrowing and shift of the particle size spectrum into the range of 0--0 µm can be observed due to the ball milling. As the particle sizes have decreased, the specific surface area has increased. Since no new oxygen is introduced, it can be hypothesised that there are oxide-free surface fractions when the specific surface area has increased. In the following section, the newly formed surfaces were examined with regard to oxidation.

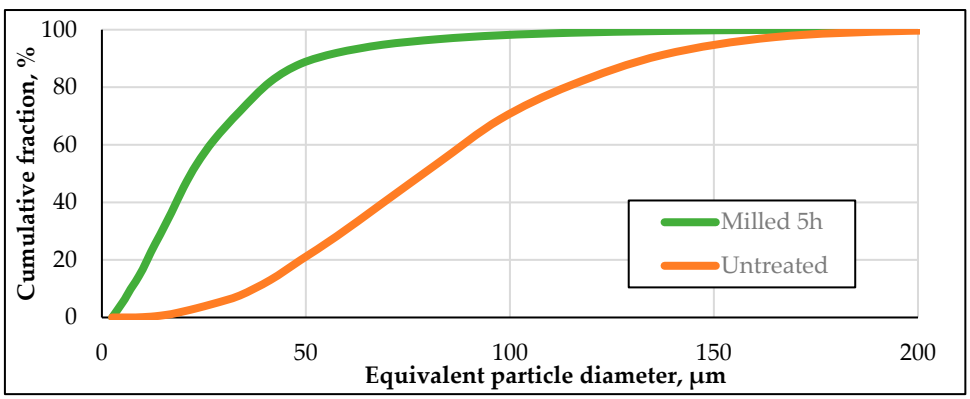

Preprints (www.preprints.org) | NOT PEER-REVIEWED | Posted: 12 July 2023 doi:10.20944/preprints202307.0801.v1

Figure 2. Particle size distribution of GE48 powder before and after milling.

3.2. X-ray Photoelectron Spectroscopy

The O1s spectra on the left side of Figure 3 show that the GEM+OX powder (milled and oxidized, process variants L85, L840) has the most metal oxides on the particle surface. Most likely this is due to the increased particle surface area after milling, which tends to reoxidise in air. The O1s signal is therefore composed of the oxide layer broken up by milling and the reoxidised particle surface. The Reference (process variant REF) powder contains a smaller amount of surface metal oxides, where the peak for organic compounds has a higher intensity than that for metal oxides. This trend continues for the OXYGEN-FREE (process variants XHV6, XHV8, V8) powder, which has the lowest amount of metal oxides in all O1 detail spectra, indicating a decrease in passivating surface oxide layers. Looking at the Ti2p detail spectra on the right side of Figure 3, there is little difference in the chemical state of the titanium species between GEM+OX and the reference sample. This is to be expected as both sample surfaces were exposed to air during fabrication and transport. The largest difference is seen in the Ti2p detail spectrum of the oxygen-free sample. Here, the amount of Ti^{2+} and Ti^{4+} species on the surface is quite similar compared to the other two powders. We assign the Ti^{2+}, Ti^{3+} and Ti^{4+} species to TiO, Ti_2O_3 and TiO_2, respectively, as observed after transporting pure Ti samples in silane-doped argon atmosphere for extended periods [24]. Silane reacts strongly with oxygen and acts as an oxygen scavenger, but this is not entirely true for water. The reaction between silane and residual water, which remains present in silane-doped argon atmospheres, is kinetically limited [27]. Consequently, the atmosphere is not able to completely prevent the oxidation of titanium, as water can also have an oxidising effect, especially on high-affinity metal surfaces such as titanium and aluminium [28,29]. Lee et al. observed the formation of uniformly distributed Ti^{2+}, Ti^{3+} and Ti^{4+} species when titanium surfaces were exposed to water, which is consistent with the XPS results discussed in this paper [30]. Overall, however, the Ti2p spectra show significant differences in the chemical composition of the surface of the oxygen-free transported sample compared to the samples transported in air. This suggests that deoxidation of the GE48 particles has indeed occurred, as it affects the surface chemistry of the powder, even when reoxidation by residual water molecules in the atmosphere is taken into account.

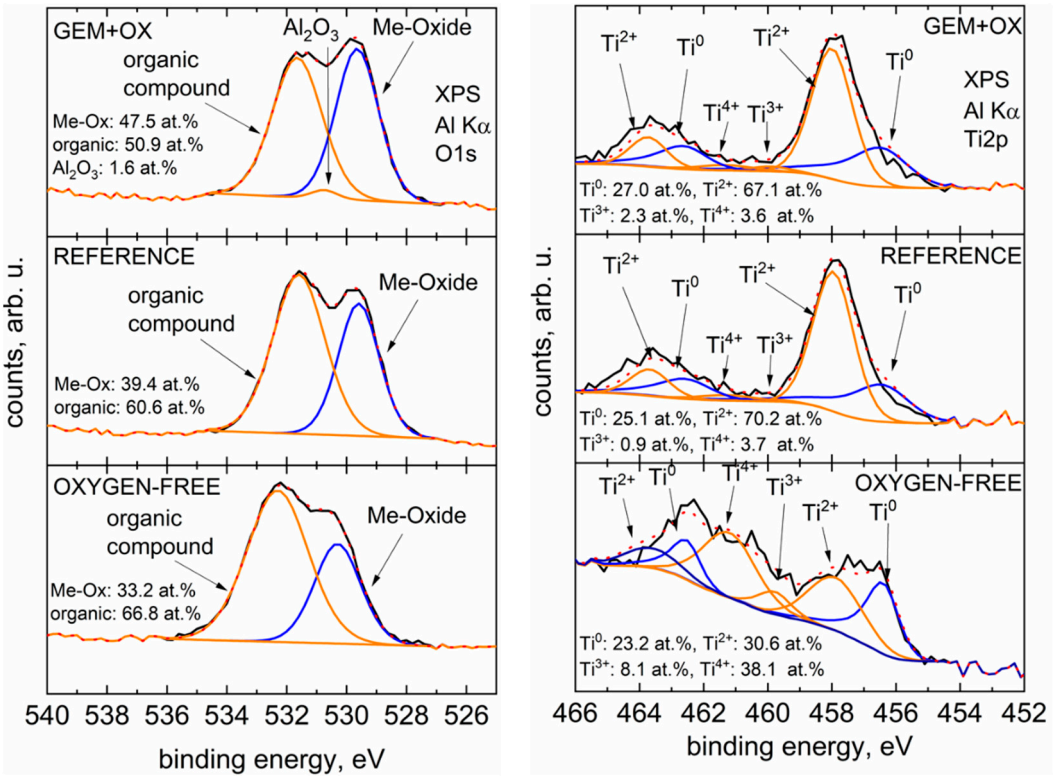

Preprints (www.preprints.org) | NOT PEER-REVIEWED | Posted: 12 July 2023 doi:10.20944/preprints202307.0801.v1

Figure 3. O1s (left) and Ti2p (right) detail spectra of the GE48 powder samples.

3.3. Pressability

By ball milling the powders, green compacts could be pressed without the need to add any pressing agent or lubricant. However, the variants L85 and L840 exposed to ambient air showed radial cracks and fragmentation after ejection from the pressing tool. Only an unstable bond could be created in the initial powder of the REF sample, which is why the transfer to the sintering furnace already led to a considerable loss of material (see Figure 4).

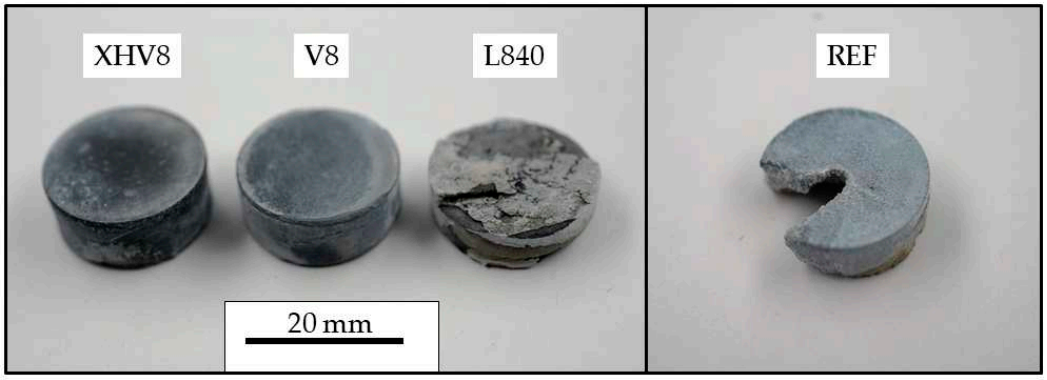

Figure 4. Specimens after pressing.

3.4. Density

The densities of the milled variants (XHV6, XHV8, V8, L85 and L840) differed only slightly from each other with an average density of 3.62 g/cm³. The density determination thus showed no clear influence of the oxygen-free processing. In comparison, the density of the reference sample was only 3.42 g/cm³, so that a density increase of 5.8 % was observed for all milled powders.

3.5. Microstructure

From the optical microscopic images of the longitudinal sections under polarised light, clear differences between the microstructures of the ground powder and the reference can be seen (Figure 5). First of all, the difference in particle size can be seen. Furthermore, there are inclusions and pores between the particles of the reference sample REF. At the same time, sinter neck formation and recrystallisation across particle boundaries were locally evident. The images of the samples show isolated pores in the microstructure. Furthermore, there are no clear differences between variants without (V8) and with oxygen contact (L840) before pressing.

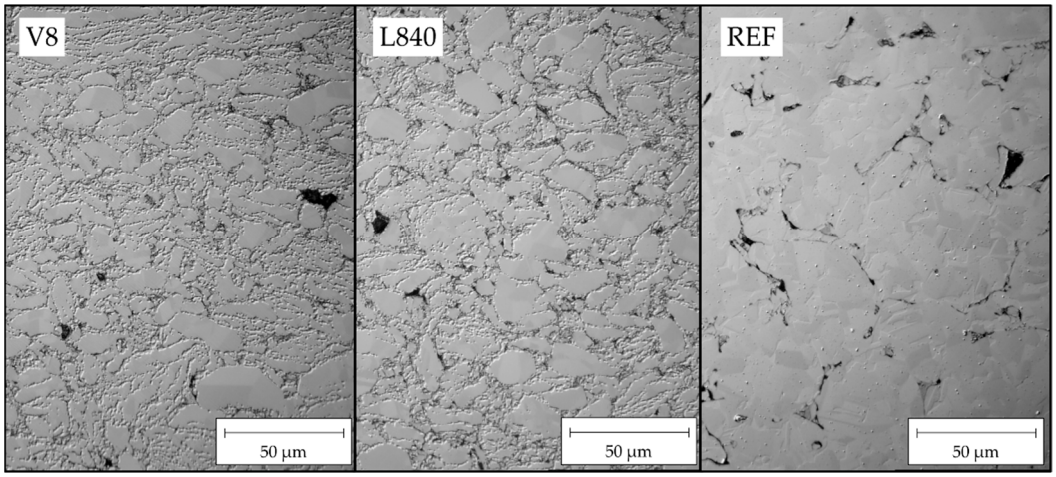

Figure 5. Images of the central area under polarized light.

Preprints (www.preprints.org) | NOT PEER-REVIEWED | Posted: 12 July 2023 doi:10.20944/preprints202307.0801.v1

Along the former particle boundaries, bands of dark pits are visible, which can be assigned to the MAX phase Ti_2AlC by EDX measurements (Figure 6). It can be assumed that the carbon input occurred during milling from the toluene used. An influence of the vacuum drying could not be determined.

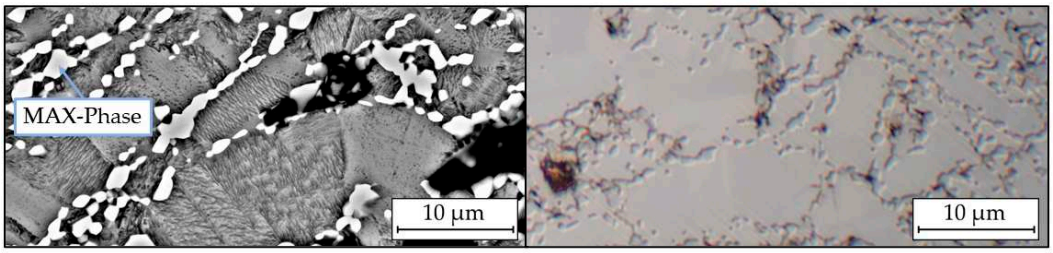

Figure 6. MAX-phase in the microstructure of XHV8.

3.6. Hardness

Based on the hardness results in Figure 6, it can be seen that a higher pressing pressure and the milling process lead to a higher hardness. For sample XHV8, there is a 15% increase in hardness compared to REF. The two samples that were exposed to the environment after milling (L85 and L840) show lower hardnesses. As sample L840 was exposed to the environment for a longer period of time, the oxide layer could be more pronounced here. On sample V8 it can be seen that vacuum drying has no influence on the hardness. The difference to sample XHV8 is within the standard deviation.

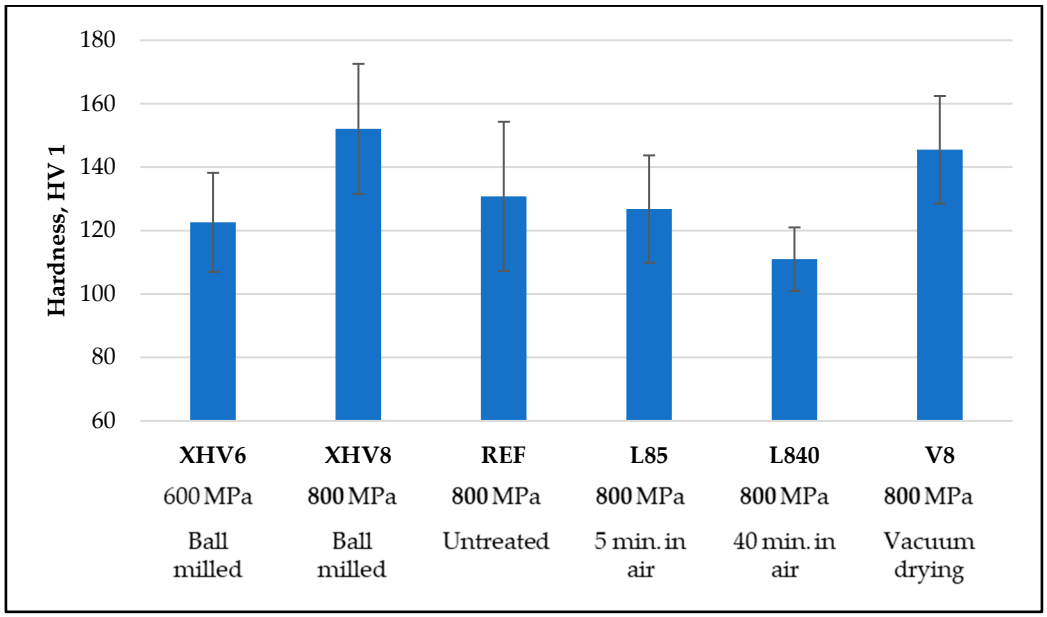

Figure 6. Hardness measurement results according to Vickers.

4. Discussion

The observations and experimental results show that the particle size is reduced during ball milling in a silane-doped atmosphere and oxide-free particle surfaces are produced and obtained. The green compacts produced from milled powder exhibit a higher density. This is attributed to the reduction in particle size. The smaller powder particles can fill voids more easily, resulting in a denser component. Therefore, a finer the microstructure of the sintered samples is achieved. The use of ball milled powder leads to a significant improvement in the pressability of the powders (see Figure 4). This indicates the creation of partially oxide-free surfaces on the powder particle. The free surfaces support the cold welding of the particles during pressing resulting in improved green strength and

reduced cracking. Furthermore, it is expected that the bare metal contact of the powder particles favours diffusion during sintering. This shows in an increase of the hardness after sintering from 130.8 HV1 to 152.1 HV1 in the oxide-free variants.

The XPS measurements have shown that exposure to air of the powder milled in the silane-doped atmosphere leads to the formation of new oxide layers on the exposed surfaces. Thus, it can be concluded that the ball milling did indeed create oxide-free surfaces which oxidized in reaction with water vapour instead of gaseous oxygen. This finding, together with the experimental results from powder processing highlights the significance of the silane-doped atmosphere. It is elementary to obtain and preserve oxide-free surfaces and to benefit from the oxide-free particle surfaces created by ball milling. Both the processing and the transport to the process steps must take place under exclusion of oxygen. The effect of ambient air on the oxygen-free milled powder has a significant negative influence on the powder compacts' green strength and thereby processability.

With the chosen sintering parameters, there were no clear effects on density and microstructure after sintering compared to completely oxygen-free processed variants. Since the thermal processes also led to the sintering of the particles in the reference sample without prior ball milling, the barrier effect of the new oxides after milling was apparently overcome during the selected sintering process. The increase in density is therefore attributed to the improved pressability of the ground powders. Thus, it can be stated that the ball milling process breaks up the oxide shards of the TiAl-powder and produces oxide-free surfaces. The silane-doped atmosphere inhibits the oxidation of the free surfaces and the oxide-free surfaces are obtained. This allows the TiAl-powder to be processed with die pressing and sintering. In the future, the changes in the powder caused by ball milling will be investigated in more detail. In particular, the mechanisms behind oxide layer break-up and the resulting opportunities for process optimization during sintering will be investigated further.

Author Contributions: Conceptualization, B.-A.B., K.B., R.G. and W.M.-F.; methodology, S.D. and M.S.; validation, K.B., J.P., J.U., S.D., R.G. and M.S.; investigation, S.D. and M.S.; writing—original draft, S.D. and M.S.; writing—review and editing, K.B., J.P., J.U., S.D., R.G. and M.S.; visualization, S.D. and M.S.; supervision, B.-A.B., K.B., J.P., J.U., W.M.-F. and R.G.; project administration, B.-A.B. and W.M.-F.; funding acquisition, B.-A.B and W.M.-F.. All authors have read and agreed to the published version of the manuscript.

Funding: Funded by the Deutsche Forschungsgemeinschaft (DFG, German Research Foundation) – Project-ID 394563137 – SFB 1368 TP A03 and TP S01.

Data Availability Statement: The data presented in this study are available in the article.

Conflicts of Interest: The authors declare no conflict of interest.

References

1. Liu, B.; Liu, Y.; Zhang, W.; Huang, J. S.: Hot deformation behavior of TiAl alloys prepared by blended elemental powders. **2011** Intermetallics 19(2), pp. 154–159.
2. Clemens, H.; Mayer, S., Design, Processing, Microstructure, Properties, and Applications of Advanced Intermetallic TiAl Alloys. **2013**, *Advanced Engineering Materials* 15, pp. 191–215.
3. Clemens, H.; Mayer, S., Heilmaier, M.: Pulvermetallurgische Herstellung von innovativen Hochtemperaturwerkstoffen. **2021**, *BHM Berg- und Hüttenmännische Monatshefte 166*, pp. 1–7.
4. Voisin, T.; Monchoux, J.-P.; Durand, L.; Karnatak, N.; Thomas, M.; Couret, A., An Innovative Way to Produce γ-TiAl Blades: Spark Plasma Sintering. **2015**, *Advanced Engineering Materials 17*, pp. 1408–13.
5. Bewlay, B. P.; Nag, S.; Suzuki, A.; Weimer, M. J., TiAl alloys in commercial aircraft engines. **2016**, *Materials at High Temperatures 33*, pp. 549–559.
6. Mogale, N.; Matizamhuka, W.: Spark Plasma Sintering of Titanium Aluminides: A Progress Review on Processing, Structure-Property Relations, Alloy Development and Challenges. **2020**, metals
7. Beiss, P., *Pulvermetallurgische Fertigungstechnik*. Heidelberg: Springer Vieweg, Berlin, Deutschland **2013**; DOI: 10.1007/978-3-642-32032-3
8. Jiao, L.; Feng, Q.; He, S.; Duan, B.; Dou, Z.; Li, C.; Lu, X.: Direct oxygen removal from titanium aluminide scraps by yttrium reduction. **2021**, Nonferrous Metals Society of China 32, pp. 2428-2437
9. Behrens, B.-A.; Bonhage, M.; Bohr, D.: Neuartige Verfahrenskombination zur Verarbeitung von Werkstoffen auf Titanaluminid-Basis unter sauerstofffreier Atmosphäre. **2020**, 23. Umformtechnisches Kolloquium Hannover.

10. Bakulin, A., V.; Hocker, S.; Kulkova, S., E.: Role of Intermediate Metal and Oxide Layers in Change of Adhesion Properties of TiAl/Al2O3 Interface. **2021**, Physical Mesomechanics, Vol. 24, No. 5, pp. 523–532
11. Attia, M.: Cold-isostatic pressing of metal powders: a review of the technology and recent developments. **2021**, Solid State and Materials Sciences
12. Bay, N.: Mechanisms Producing Metallic Bonds in Cold Welding. **1983**
13. Pflumm, R.; Friedle, S.; Schütze, M.: Oxidation protection of g-TiAl-based alloys e A review. **2014,** Intermetallics 56 (2015), pp. 1-14
14. Gökce, A.; Findik, F.: Mechanical and physical properties of sintered aluminum powders. *Journal of Achievments in Materials and Manufacturing Engineering* **2008**, pp. 157–64.
15. Mphahlele, M. R.; Olubambi, P. A.; Olevsky, E. A.: Advances in Sintering of Titanium Aluminide: A Review. **2023**, JOM
16. Gerling, R.; Clemens, H.; Schimansky, F. P.: Powder Metallurgical Processing of Intermetallic Gamma Titanium Aluminides, **2004**, pp. 23–38.
17. Meier, G., H.; Pettit, F., S.; Hu, S.: Oxidation behavior of titanium aluminides. **1993**, Journal de Physique, pp. 395-402
18. Diaz, M., R.; Szafarska, M.; Gustus, R.; Möhwald, K.; Maier, H., J.: Oxide Free Wire Arc Sprayed Coatings—An Avenue to Enhanced Adhesive Tensile Strength. **2022**, metals
19. Holländer, U.; Wulff, D.; Langohr, A.; Möhwald, K.; Maier, H., J.: Brazing inSiH 4-Doped Inert Gases: A New Approach to an Environment Friendly Production Process. **2019**, International Journal of Precision Engineering and Manufacturing-Green Technology
20. Murty, B., S.; Rao, M., M.; Ranganthan, S.; Milling maps and amorphization during mechanical alloying. **1994**, Acta metall Mater Vol. 43, No. 6, pp. 2443-2450
21. Mogale, N., F.; Matizamhuka, W., R.: Spark Plasma Sintering of Titanium Aluminides: A Progress Review on Processing, Structure-Property Relations, Alloy Development and Challenges. **2020**, metals
22. Shengguan, Qu; Xiaoqiang, Li; Yuanyuan, Li; Lianxi, Hu; Erde, W.: Manufacturing a TiAl alloy by high-energy ball milling and subsequent reactive sintering. **2006**, Rare Metals Vol.25
23. Behrens, B., A.; Brunotte, K.; Peddinghaus, J.; Heymann, A.; Influence of dwell time and pressure on SPS process with tita-2 nium aluminides. **2021**, metals
24. Gustus, R.; Szafarska, M.; Maus-Friedrichs, W.: Oxygen-free transport of samples in silane-doped inert gas atmospheres for surface analysis. **2021**, Journal of Vacuum Science & Technology B, 39, 54204, DOI: 10.1116/6.0001180
25. Scofield, J., H.: Hartree-Slater subshell photoionization cross-sections at 1254 and 1487 eV. **1975**, Journal of Electron Spectroscopy and Related Phenomena
26. Reilman, R., F.; Msezane, A.; Manson, S., T.; Relative intensities in photoelectron spectroscopy of atoms and molecules. **1976**, Journal of Electron Spectroscopy and Related Phenomena
27. Szafarska, M., Gas Phase Reaction of Silane with Water at Different Temperatures and Supported by Plasma, *ACS 2023*
28. Maier, H., J.; Herbst, S., Denkena, B.; Dittrich, M., A.; Schaper, F.; Worpenberg, S.; Gustus, R.; Maus-Friedrichs, W.: Towards Dry Machining of Titanium-Based Alloys: A New Approach Using an Oxygen-Free Environment. **2020**, metals
29. Barienti, K.; Werwein, S.; Herbst, S.; Maier, H., J.; Nürnberger, F.: A novel way to reduce the critical deformation for cold roll bonding. **2023**
30. Lee, P.A., Oxide formation on Fe and Ti thin films and on Fe thin films modified with ultrathin layers of Ti, *Surface and Interface Analysis 1991*